



**HAL**  
open science

## **Nd:YAG single-crystal fiber as power amplifier of pulses below one nanosecond**

Igor Martial, François Balembois, Julien Didierjean, Patrick Georges

► **To cite this version:**

Igor Martial, François Balembois, Julien Didierjean, Patrick Georges. Nd:YAG single-crystal fiber as power amplifier of pulses below one nanosecond. *Optics Express*, 2011, 19 (12), pp.11667-11679. 10.1364/OE.19.011667 . hal-00819340

**HAL Id: hal-00819340**

**<https://hal-iogs.archives-ouvertes.fr/hal-00819340>**

Submitted on 20 Nov 2015

**HAL** is a multi-disciplinary open access archive for the deposit and dissemination of scientific research documents, whether they are published or not. The documents may come from teaching and research institutions in France or abroad, or from public or private research centers.

L'archive ouverte pluridisciplinaire **HAL**, est destinée au dépôt et à la diffusion de documents scientifiques de niveau recherche, publiés ou non, émanant des établissements d'enseignement et de recherche français ou étrangers, des laboratoires publics ou privés.

# Nd:YAG single-crystal fiber as high peak power amplifier of pulses below one nanosecond

Igor Martial,<sup>1,2,\*</sup> François Balembois,<sup>1</sup> Julien Didierjean,<sup>2</sup> and Patrick Georges<sup>1</sup>

<sup>1</sup>Laboratoire Charles Fabry de l'Institut d'Optique, CNRS, Université Paris-Sud, Campus Polytechnique, RD 128, 91127 Palaiseau Cedex, France

<sup>2</sup>Fibercryst SAS, La Doua-Bâtiment l'Atrium, Boulevard Latarjet, F- 69616 Villeurbanne Cedex, France

\*i.martial@fibercryst.com

**Abstract:** We explore the potential of Nd:YAG single-crystal fibers for the amplification of passively Q-switched microlasers operating below 1 ns. Different regimes are tested in single or double pass configurations. For high gain and high power amplification this novel gain medium provided average powers up to 20 W at high repetition rate (over 40 kHz) for a pulse duration of 1 ns. As an energy amplifier, Nd:YAG single-crystal fiber delivered 2.7 mJ, 6 MW 450 ps pulses at 1 kHz. The extraction efficiencies vary from 8% to 32.7% following the configurations.

©2011 Optical Society of America

**OCIS codes:** (140.3480) Lasers, diode-pumped; (140.3530) Lasers, neodymium; (140.3380) Laser materials; (060.2290) Fiber materials; (140.3280) Laser amplifiers; (140.3540) Lasers, Q-switched.

---

## References and links

1. M. Tsunekane, T. Inohara, A. Ando, N. Kido, K. Kanehara, and T. Taira, "High peak power, passively Q-switched microlaser for ignition of engines," *IEEE J. Quantum Electron.* **46**(2), 277–284 (2010).
2. P. Peuser, W. Platz, and G. Holl, "Miniaturized, high-power diode-pumped, Q-switched Nd:YAG laser oscillator-amplifier," *Appl. Opt.* **50**(4), 399–404 (2011).
3. F. Druon, F. Balembois, P. Georges, and A. Brun, "High-repetition-rate 300-ps pulsed ultraviolet source with a passively Q-switched microchip laser and a multipass amplifier," *Opt. Lett.* **24**(7), 499–501 (1999).
4. Y. Isyanova, J. G. Manni, and D. Welford, "High-power, passively Q-switched microlaser - power amplifier system," in *Advanced Solid-State Lasers*, C. Marshall, ed., Vol. 50 of OSA Trends in Optics and Photonics (Optical Society of America, 2001), paper MD2.
5. S. Forget, F. Balembois, P. Georges, and P.-J. Devilder, "New 3D multipass amplifier based on Nd:YAG or Nd:YVO<sub>4</sub> crystals," *Appl. Phys. B* **75**(4-5), 481–485 (2002).
6. J. G. Manni, "Amplification of microchip oscillator emission using a diode-pumped wedged-slab amplifier," *Opt. Commun.* **252**(1-3), 117–126 (2005).
7. A. Agnesi, P. Dallochio, S. Dell'Acqua, F. Pirzio and G. Reali, "High peak power sub-nanosecond MOPA laser," presented at 4th EPS-QEOD EUROPHOTON CONFERENCE, Hamburg, September 2010, paper WeB5.
8. A. Gaydardzhiev, D. Draganov, and I. Buchvarov, "A compact Nd:YAG slab amplifier for miniature solid state Q-switched lasers," presented at 4th EPS-QEOD EUROPHOTON CONFERENCE, Hamburg, September 2010, paper WeP18.
9. C. D. Brooks and F. Di Teodoro, "1-mJ energy, 1-MW peak-power, 10-W average-power, spectrally narrow, diffraction-limited pulses from a photonic-crystal fiber amplifier," *Opt. Express* **13**(22), 8999–9002 (2005).
10. F. Di Teodoro and C. D. Brooks, "Multi-MW peak power, single transverse mode operation of a 100 micron core diameter, Yb-doped photonic crystal rod amplifier," *Fiber Lasers IV: Technology, Systems, and Applications*, edited by D. J. Harter, A. Tünnermann, J. Broeng, C. Headley III, Proc. of SPIE Vol. **6453**, 645318, (2007).
11. R. L. Farrow, D. A. V. Kliner, P. E. Schrader, A. A. Hoops, S. W. Moore, G. R. Hadley, and R. L. Schmitt, "High-peak-power (>1.2 MW) pulsed fiber amplifier," *Fiber Lasers III: Technology, Systems, and Applications*, edited by A. J. W. Brown, J. Nilsson, D. J. Harter, A. Tünnermann, Proc. of SPIE Vol. **6102**, 61020L, (2006).
12. A. Galvanuskas, M. Cheng, K. Hou, and K. Liao, "High peak power pulse amplification in large-core Yb-doped fiber amplifier," *IEEE J. Sel. Top. Quantum Electron.* **13**(3), 559–566 (2007).
13. J. Didierjean, M. Castaing, F. Balembois, P. Georges, D. Perrodin, J. M. Fourmigué, K. Lebbou, A. Brenier, and O. Tillement, "High-power laser with Nd:YAG single-crystal fiber grown by the micro-pulling-down technique," *Opt. Lett.* **31**(23), 3468–3470 (2006).
14. J. Dong, A. Rapaport, M. Bass, F. Szipocs, and K. Ueda, "Temperature-dependent stimulated emission cross section and concentration quenching in highly doped Nd<sup>3+</sup>: YAG crystals," *Phys. Status Solidi., A Appl. Mater. Sci.* **202**(13), 2565–2573 (2005).
15. S. Guy, C. L. Bonner, D. P. Shepherd, D. C. Hanna, A. C. Tropper, and B. Ferrand, "High-inversion densities in Nd:YAG: upconversion and bleaching," *IEEE J. Quantum Electron.* **34**(5), 900–909 (1998).

16. A. Rapaport, S. Z. Zhao, G. H. Xiao, A. Howard, and M. Bass, "Temperature dependence of the 1.06-microm stimulated emission cross section of neodymium in YAG and in GSGG," *Appl. Opt.* **41**(33), 7052–7057 (2002).
  17. O. Kimmelma, I. Tittonen, and S. C. Buchter, "Thermal tuning of laser pulse parameters in passively Q-switched Nd:YAG lasers," *Appl. Opt.* **47**(23), 4262–4266 (2008).
  18. N. P. Barnes and B. Walsh, "Amplified Spontaneous Emission –Application to Nd:YAG Lasers," *IEEE J. Quantum Electron.* **35**(1), 101–109 (1999).
  19. A. E. Siegmann, *Lasers* (University Sciences Books, 1986) p 386.
  20. W. Koechner, *Solid State Laser Engineering*, 5th ed. (Springer, 1999).
- 

## 1. Introduction

Passively Q-switched Nd:YAG microlasers represent a simple way to produce subnanosecond pulses in a very compact design. At low repetition rate (10 Hz), 2.7 mJ pulses with a peak power of more than 5 MW have already been generated [1]. The MOPA (Master Oscillator Power Amplifier) configuration can extend the performance and 8.4 mJ pulses have recently been demonstrated [2] with a single pass Nd:YAG amplifier operating at 25 Hz. Those lasers can address applications requiring high energy and high peak power pulses such that ignition of engines or airborne/space borne lidar systems. However, the low repetition rate is a drawback for material processing or high precision ranging and imaging where the speed is a key parameter. Those applications require repetition rates ranging from 1 kHz to 100 kHz and a combination of high peak power (MW level) and high average power (watt level) with an energy reaching the millijoule level. Passively Q-switched microlasers cannot address it directly since the average power is generally limited to hundreds of milliwatts and the peak power to hundreds of kilowatts. Amplification stages are then needed. The amplifiers for Nd doped microlasers can be sorted in two parts: the bulk amplifiers and the fiber amplifiers.

Diode-pumped Nd doped crystals are used since years for the amplification stage of the short pulse passively Q-switched microlaser. Nd:YVO<sub>4</sub> is generally preferred to Nd:YAG [3–7] because of its higher emission cross section. The amplifiers are generally multipass systems [3–6] or used several gain media [7]. This last case gives the best results in energy (1 mJ) and average power (10 W) but with a limited extraction efficiency (8%). Nd:YAG is even so interesting for the amplification of microlasers operating at low repetition rate (1 kHz) since the energy storage is 2.3 times higher than in Nd:YVO<sub>4</sub>. Following this idea, a Nd:YAG 5-pass amplifier has been recently carried out [8] with an output energy of 0.9 mJ for a repetition rate of 1 kHz corresponding to an energy extraction efficiency of 6.5%.

Passively Q-switched Nd:doped microlasers are also amplified by double clad Yb doped fibers. The systems developed used large core fibers (either photonic crystal fibers [9,10] or large mode area (LMA) fibers [11,12]) in order to limit the nonlinear effects produced by the high peak power pulses during the amplification process. The performance are impressive, with energy of 4.3 mJ and average power of 40 W [10] and peak powers up to 6 MW (even if this peak power is obtained at 50 Hz) [12]. The seeded wavelength is generally 1064 nm or 1062 nm, significantly shifted from the 1030 nm peak gain cross section of Yb:glass. In order to avoid strong amplified spontaneous emission, it was necessary to split the amplification in two fibers or more (typical core diameters are 30 μm for the first fiber amplifier and 80 μm to 100 μm for the second one) separated by a band pass filter. The only system using a single fiber amplifier is the one developed by [11]. In this case, the performance are limited to an energy of 0.67 mJ and a peak power of 1.27 MW. At this power level, authors reported temporal and spectral deformations of the pulses [9–11] induced by self-phase modulation or Raman scattering. Moreover, the energy fluence at the output of the last amplifier is huge, reaching tens of J/cm<sup>2</sup> [12]. Even if this problem can be managed with end caps, it has to be addressed specifically, increasing the complexity of the design. These different results show that the fiber amplifiers have rapidly reached their limit with MW and mJ subnanosecond amplified pulses.

On the opposite, bulk crystals are definitely not so sensitive to nonlinear effects since the beam size is generally much larger (a few hundreds of μm) but the performance demonstrated in the past are clearly lower than the one obtained with fibers. In this paper, we demonstrate

that the potential of Nd:YAG has not been fully exploited and that it can equal and even overcome the performance of the fiber amplifiers for subnanosecond pulses, providing to find the right geometry for the crystal. For that, we use Nd:YAG single-crystal fibers [13]. This paper reports the performance of this particular gain medium for various seeds, repetition rates, powers and energies, and for two pulse duration: 0.45 ns and 1 ns. Firstly (section 2) we present the interest to use a Nd:YAG single-crystal fiber for amplification. Next (section 3), we present the different architectures developed and the amplifier performance for a high repetition rate (up to 100 kHz) passively Q-switched microlaser. Then (section 4.) we report the performance of the Nd:YAG crystal fiber amplifier as high power amplifier. We study the amplification of high energy (several mJ), high peak power pulses in section 5. Finally (section 6), we comment the performance obtained and the advantages of single crystal fibers over existing bulk and fiber amplifiers.

## 2. Interest of Nd:YAG single-crystal fiber for pulse amplification

As previously reported [13], single-crystal fibers are long (typically 50 mm) and thin (typically <1 mm diameter) rods able to confine the pump beam by guiding and able to propagate the signal beam in free space without guiding or diffraction. The main advantage of single-crystal fiber is the low doping concentration (typically 0.2% in Nd) whereas the typical doping level is about 1% in bulk Nd doped crystal [3,5,7,8]. At this doping level, numerous effects may limit the gain of the amplifier. As Nd:YAG laser medium operating at 1064 nm and pumped at 808 nm is a four level system, the gain coefficient is simply the product of the emission cross section by the population density of the upper state level. Therefore, the gain limitation may come from those two quantities.

Gain limitation occurs firstly on the population inversion density  $n_2$ . A 1% doping level is low enough to neglect the fluorescence quenching [14] but it is still high enough to have important limitation through the effect of upconversion. As explained in [15] up-conversion empties the excited state by a rate  $\gamma n_2^2$ ,  $\gamma$  being the up-conversion parameter. In a 1% doped medium, the pump absorption is high and creates a high population inversion density leading in the same time to important leakages from the excited state by up-conversion. This effect is all the more pronounced as the up-conversion parameter increases with the doping level. Moreover, it reduces not only the population of the upper level but also induces a local increase of temperature since it is a non radiative process.

This leads to the second limitation of the gain: the emission cross section decreases and shifts with the temperature [16]. Temperature increase can be managed by a good transfer coefficient between the crystal and its heatsink but it is intrinsically related to the quantum defect between the pump and the signal, the up-conversion process and the absorption coefficient. In a 1% doped Nd:YAG crystal, the temperature can easily reach 50-100°C on the pumped face because the absorption coefficient is relatively high ( $4 \text{ cm}^{-1}$  typically for a diode pumping at 808 nm). Whereas the peak emission cross section decrease is around 10% for this range of temperature increase, the spectral shift around  $4.8 \text{ pm}/^\circ\text{C}$  [17] can have an important effect on the gain: assuming a spectral linewidth of 0.45 nm for Nd:YAG at 1064 nm, the laser seed can be out of the gain curve of the amplifier at 100°C.

In a low doped Nd:YAG crystal, all those effects are reduced: the population inversion density  $n_2$  and the up-conversion parameter  $\gamma$  are lower. The temperature increase is limited by the low absorption and the reduction of non radiative effects (concrete illustration of these effects are given at the end of this section). The low doping concentration is the main advantage of single-crystal fibers. However, one problem comes from the overlap between the pump and the signal in the crystal. For signal beams in the order of hundreds of  $\mu\text{m}$  diameter, as it is the case in neodymium doped bulk amplifiers, one can neglect the size evolution of the signal along the amplifier length. This is not the case for the pump beam. As an example, a pump beam coming from a fiber coupled laser diode (with a typical  $M^2$  of 40, corresponding to the state of the art for high power lasers diodes) has a Rayleigh range of approximately 7 mm in Nd:YAG when focused on a 200  $\mu\text{m}$  radius (corresponding to the experiments presented in this paper). Therefore, a classical design for longitudinal pumping systems leads

to use a crystal length in the order of the pump Rayleigh range to ensure a good overlap between the pump beam and the signal beam. The crystal must be sufficiently doped to ensure absorption: in our example, a 1% doped 7 mm long crystal will provide an absorption of approximately 90% at 808 nm. In our low-doped single-crystal fiber (0.2% doped), a length five times higher than the pump Rayleigh range is required provide the same absorption.

Here comes the second advantage of the single-crystal fiber: as the diameter of the gain medium is low (typically 1 mm or even below), the pump beam remains confined close to the signal beam by total internal reflection on the rod surface. The overlap between the pump and the signal is then increased. The small diameter of the crystal is also a way to reduce the temperature increase inside the gain medium since the heatsink is closer to the source of heating. This contributes to avoid gain reduction via spectral shifting in case of Nd:YAG.

To illustrate this discussion, we compared the performance of a 0.2% Nd:YAG single-crystal fiber with other Nd:YAG crystals with different doping concentrations and different geometries in the same amplification setup described on the Fig. 1. The pump diode is a 60 W fiber coupled laser diode at 808 nm (100  $\mu\text{m}$  core diameter, NA 0.22). The Nd:YAG gain media are longitudinally pumped and long enough to ensure a pump absorption of more than 90%. The signal beam is injected in the gain medium through a dichroic mirror in a co-propagating way with respect to the pump beam. For the experiments presented in this paper, we used several passively Q-switched (PQS) microlasers operating at different repetition rates (from 1 kHz to 100 kHz) and with different output powers (more completely described in the next sections). The measurements presented in this section were collected during the different experiments.

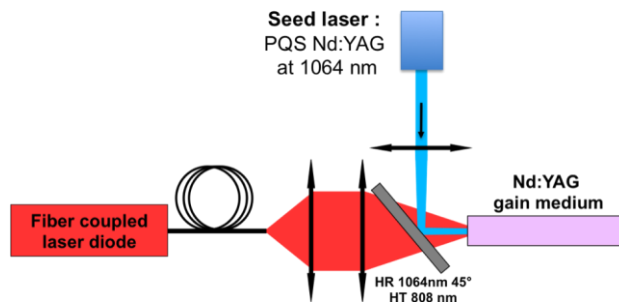


Fig. 1. Experimental setup for the test of the amplifiers.

In the setup described on the Fig. 1, the gain is measured after a single pass through the Nd:YAG media by the ratio between the output average power to the input average power. The Fig. 2 gives the gain versus the pump power. The 1% Nd crystal (square section of 3 mm by 3 mm) was pumped at a maximum of 20 W in order to avoid crystal fracture. It shows a roll-over at a pump power of 10 W that can be interpreted by the combined effects of up-conversion, local temperature increase and spectral gain shifting. In order to limit those effects, we tested a 0.5% Nd doped composite rod with a first undoped section of 2 mm and with a smaller diameter of 2 mm. The roll-over occurred at significantly higher pump power (around 35 W) but it was still here, despite the better cooling geometry. At maximum pump power, the gain was completely lost. With a 0.3% doping and a rod diameter of 1.5 mm, the roll-over was shifted towards power of more than 60 W but the gain increase was considerably limited at power higher than 40 W. Finally, the 0.2% 1 mm diameter single-crystal fiber presented no roll-over and the highest gain with a nice exponential increase (except for the last point) and despite a higher saturation caused by a higher input signal (see Fig. 1 legend). This 50 mm long crystal fiber (provided by Fibercryst SAS, module TARANIS) was used for all the experiments presented in the following sections.

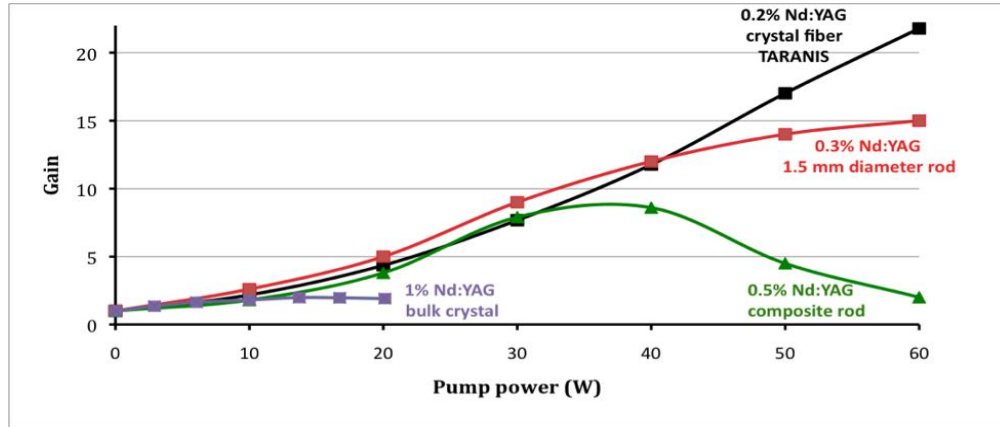


Fig. 2. Gain obtained in single pass amplification for different doped Nd:YAG media. The pump beam and signal beams have a diameter around  $400\mu\text{m}$  at the focus. The input average power is: 58 mW (1% Nd), 100 mW (0.5% Nd), 200 mW (0.3% Nd) and 260 mW (0.2% Nd single-crystal fiber).

In order to evaluate the effect of the spectral gain shift, we imaged the fluorescence emitted by the pumped face of the gain media on a high resolution optical spectrum analyzer (resolution of 0.07 nm). The experiment was carried out for the 1% doped Nd:YAG crystal and for the 0.2% Nd:YAG crystal fiber at different pump powers. The Fig. 3 shows that the spectrum is considerably shifted for the 1% doped Nd:YAG even with a moderate pump power (20W). As the spectrum of the seeding laser is also reported on the Fig. 3, we can see clearly that the signal is no more at the gain peak when the 1% Nd:YAG crystal is pumped at 20 W. The spectral shift existed also for the 0.2% Nd:YAG single-crystal fiber but it was very moderate.

Assuming a spectral shift of  $4.8\text{ pm}/^\circ\text{C}$ , we can estimate a temperature increase of  $26^\circ\text{C}$  for the single-crystal fiber and of  $106^\circ\text{C}$  for the 1% Nd:YAG. This low temperature increase for the single-crystal fiber is the key point for efficient laser amplification. Note also that the full width at half maximum is narrowed by 50% for the single-crystal fiber at 60 W whereas it is broadened by 25% in the case of the 1% doped Nd:YAG. In the first case, we attributed this spectral narrowing to the presence of amplified spontaneous emission collected by the spectrometer. In the second case, we attributed the spectral broadening to the strong temperature increase.

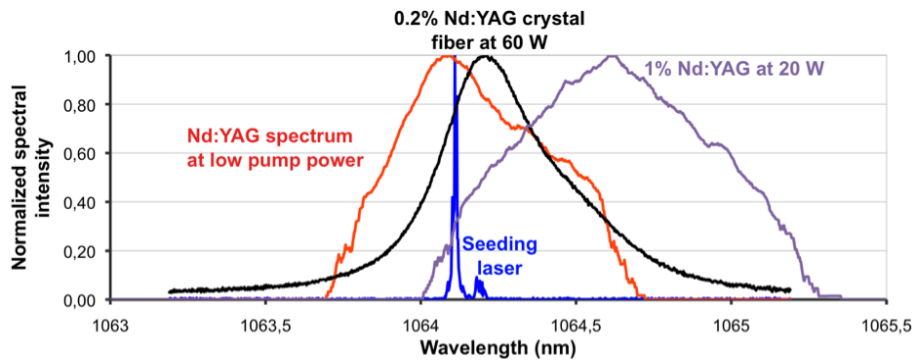


Fig. 3. Normalized fluorescence spectrum recorded at different pump powers for 0.2% doped Nd:YAG crystal fiber and for 1% doped Nd:YAG. The spectrum of the seeding laser is also added on the graph. The spectra at low pump power and for the 1% Nd:YAG are more noisy than the spectrum of the 0.2% Nd crystal fiber because the amount of spontaneous emission was much lower.

### 3. Amplification of a high repetition rate microlaser

In this section, we report the results obtained with a microlaser emitting 1 ns pulses at a repetition rate of 100 kHz and with an average power of 350 mW (provided by Teem Photonics, France). We tried two different configurations in one pass or two passes, following the propagation direction of the signal with respect to the pump axis. In the setup 1 (Fig. 4), the signal and the pump propagated in the same direction for the first pass. In the setup 2 (Fig. 5), the signal was in counter-propagation for the first pass. In both cases, the signal was collimated by a lens ( $f = 100$  mm) at the output of the microlaser. It passed then through an optical isolator, a half-wave plate and a polarizer. The half-wave plate was used to vary the signal power injected in the amplifier. The signal was then focused to a diameter of  $340 \mu\text{m}$  in the Nd:YAG single-crystal fiber by a lens ( $f = 500$  mm). The single-crystal fiber faces were antireflection coated at 808 nm and 1064 nm. For the second pass, we used a concave mirror ( $R = 200$  mm) and a quarter-wave plate to rotate the polarization of the signal by  $90^\circ$ . The output in double pass was then achieved by reflection on the polarizer. The mirror was mounted on a translation stage in order to adjust the beam size in the second pass. The transmission of the optical chain was 70% for the first pass and 63% after the second pass (without pumping). The main losses were caused by the optical isolator.

The Nd:YAG single crystal fiber used was a TARANIS-Nd module provided by Fibercryst, consisting of a 50 mm long single crystal Nd:YAG fiber having a diameter of 1 mm and its cooling system. Both faces of the single crystal fiber were anti-reflection coated at 808 nm and at 1064 nm. The transmission was measured to be 98% at 1064 nm and was independent on the position of the beam inside the single crystal fiber providing the beam was not diffracted by the edges of the crystal. The roughness of the barrel polish was 60 nm RMS. The guiding efficiency was measured in a preliminary experiment with a probe beam at 633 nm strongly focused at the input of the single crystal fiber: we found a guiding transmission of 97%. Those tests prove that the single crystal fiber is of excellent optical quality and that the barrel interface is able to guide the pump beam by total internal reflections.

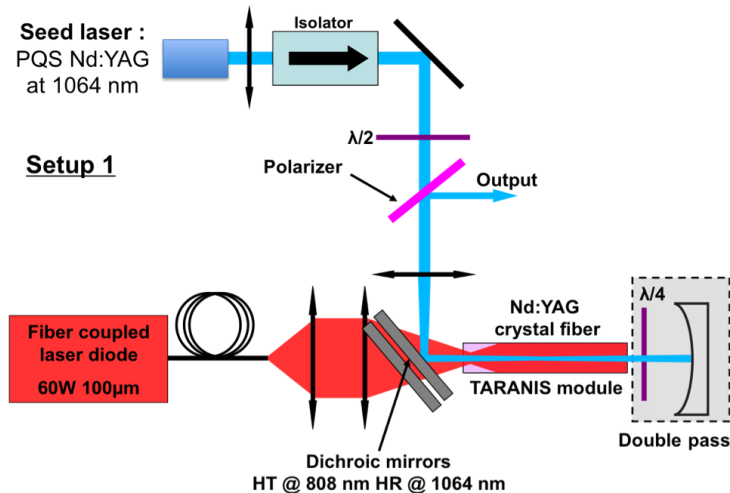


Fig. 4. Experimental setup 1: this first pass is in co-propagation, the second pass is in counter-propagation. The seed laser emitted 1 ns pulses at 100 kHz with an average power of 350 mW.

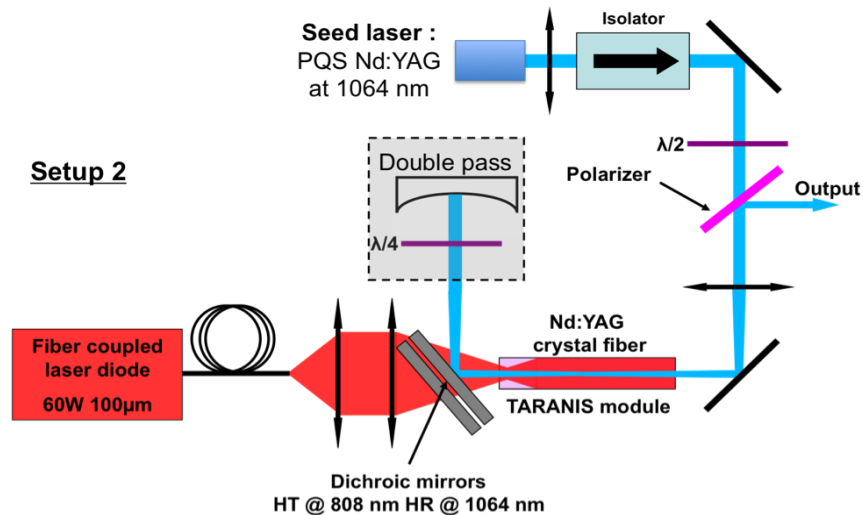


Fig. 5. Experimental setup 2: this first pass is in counter-propagation, the second pass is in co-propagation. In this section, the seed laser emitted 1 ns pulses at 100 kHz with an average power of 350 mW. It will be replaced by other seed lasers in the sections 4 and 5.

The module was regulated at a temperature of 10°C. The pump beam was imaged in the crystal fiber by a 1:4 telescope consisting of two AR coated doublets with focal lengths of 50 mm and 200 mm respectively. It led to a 400 µm diameter beam at the focus point inside the crystal. In order to protect the diode from the amplified signal, we added a second dichroic mirror, parallel to the first one. The transmission of the all pump optics was then 90%. In order to maximize the output power, the focus point of the pump beam was put slightly inside the single-crystal fiber, close to the pumped face.

In order to evaluate the propagation of the pump beam through the single crystal fiber, we used a ray tracing software associated with Monte Carlo calculations giving maps of intensity at each position in the single crystal fiber. The propagation of the pump beam (assuming no absorption) is shown on the Fig. 6. The pump beam was in free space propagation in the first 30 mm of the single crystal fiber. It was then guided by total internal reflections. Note that because of cylindrical symmetry of the crystal fiber, the pump intensity remained important in the vicinity of the propagation axis, even after total internal reflections. This is a key point for the overlap between the signal and the pump power deposited in the crystal.

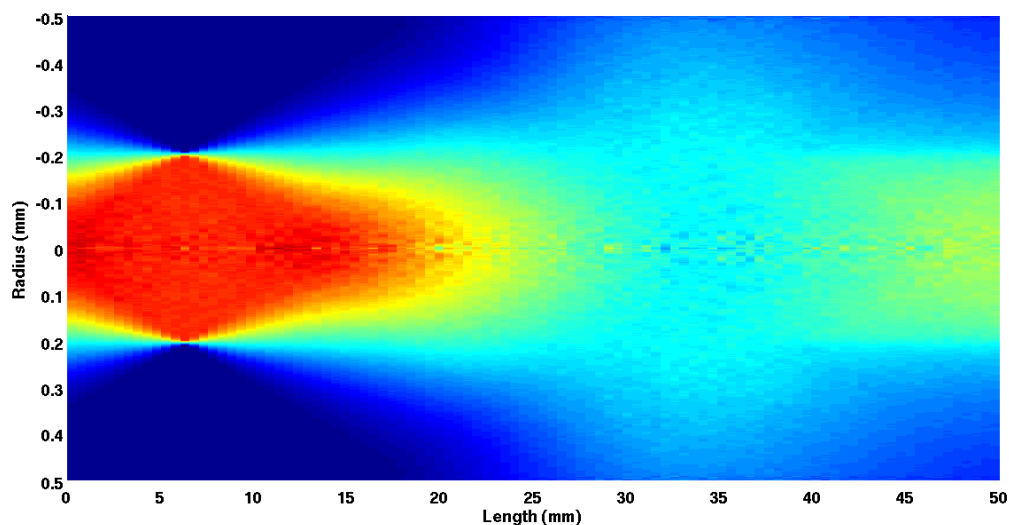


Fig. 6. Propagation of the pump beam in the single crystal fiber (assuming no absorption).

The output power after amplification is reported on the Fig. 7. Both setups gave approximately the same results: the Nd:YAG single crystal fiber can be used indifferently in co- or in counter-propagation. This shows the flexibility of the amplifier. We obtained an output power of 5.4 W in single pass (corresponding to a gain of 22) and an output power of 12.5 W in double pass (corresponding to a total gain of 57). The  $M^2$  was 1.2 at the input of the crystal fiber (before the first pass). It was measured at 1.4 for the maximum pump power after two passes in the gain medium. The pulse duration remained unchanged at 1 ns.

In single pass configurations, the output beam was linearly polarized with a ratio better than 95%. In double pass configurations, the output beam was 100% linearly polarized since the output was obtained by reflection on a polarizer. It was however possible to measure the thermal depolarization induced by the pumping after two passes in the Nd:YAG single crystal fiber by measuring the leakage power on the first polarizer of the isolator (not represented on the figures). It varied from 0 (no depolarization was observed without pumping) to 7.7% of the output power at maximum pump power (setup 2).

We measured the signal beam size in the output plan of the crystal fiber (face opposite to the pump). Without pumping, in double pass configuration (setup 2), the beam diameter was 480  $\mu\text{m}$ . At maximum pump power, the beam diameter was reduced to 200  $\mu\text{m}$  because of the thermal lens induced by the pumping.

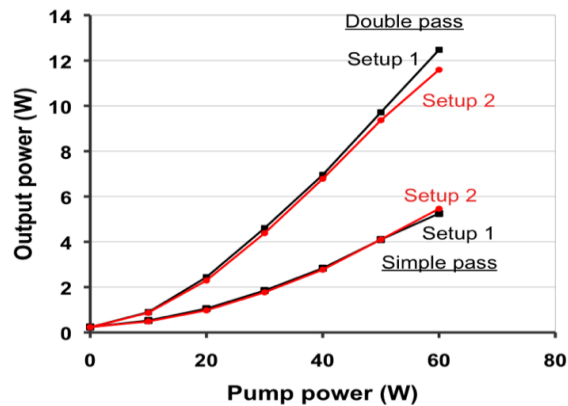


Fig. 7. Output power after one pass or two passes in the single-crystal fiber versus the pump power. The results in red are for the setup 1 and in black for the setup 2.

As the gain was high, we also carefully looked after parasitic laser effects or amplified spontaneous emission (ASE) without signal injection. In single pass configurations, no parasitic laser effect was observed. We monitored the ASE around 1064 nm by imaging the pumped face of the crystal fiber on the input of an optical spectrum analyzer. The Fig. 8 shows a linear increase of the ASE versus the pump power up to 40 W. An exponential increase is clearly visible for pump powers between 40 W and 60 W, which is the signature of ASE [18]. However, the amount of amplified spontaneous emission was not measurable with a power meter sensitive to the mW level.

In double pass configurations, we observed a laser effect between the concave mirror of the double pass system and the opposite face of the Nd:YAG single-crystal fiber producing a few watts. This effect disappeared as soon as we injected a signal in the amplifier.

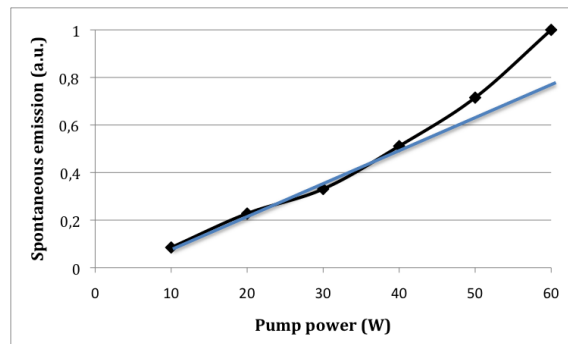


Fig. 8. Spontaneous emission collected from the pump face versus the pump power.

#### 4. Nd:YAG single-crystal fiber as a power amplifier

In order to test the potential of the Nd:YAG crystal fiber as power amplifier, we used a laser seeding source providing a higher average power: a PicoSpark™ laser source (from Teem Photonics) emitting 1 ns, 42 kHz, 120 μJ pulses with an average power of 5 W. The experiment used the same configuration as the setup 2. The Fig. 9 shows the output average power as a function of the incident pump power in a single pass configuration. We obtained more than 20.5 W for an incident pump power of 60 W, corresponding to a pulse energy of 490 μJ. With more than 15.5 W extracted from the amplifier, the efficiency was higher than 25%. The pulse duration remained at 1 ns without any deformation. The corresponding peak-

power was 490 kW. The  $M^2$  factor of the beam injected in the single-crystal fiber was 1.2. After amplification, the  $M^2$  factor stood below 1.4 (Fig. 8).

Note that the thermal lens in this single pass configuration with counterpropagating pumping has only a small influence on the signal beam size inside the Nd:YAG crystal since its effect occur only at the end of the amplification process. This can explain why the efficiency was better in this configuration than in the second pass of the previous experiment: for the same incident signal power (5W after the first pass), the output power was limited to 12 W (Fig. 7) because of reduction of the beam diameter induced by the thermal lens.

The output performance was compared to simulations. For that, we computed the gain coefficient at each position in the single crystal fiber, taking the temperature shifting of the emission cross section and the pump propagation in account. The Fig. 9 shows that the calculated output power is very close to the experimental points. In order to evaluate the contribution of the single crystal fiber end to the amplification (where the pump started to be guided), we computed the output power for a 30 mm long Nd:YAG (green line on Fig. 8). This proves that the end of the single crystal fiber contributed for 25% of the total amount of output power at maximum pump power. The simulation can also give an estimation of the overlap between the signal beam and the pump deposited in the single crystal fiber: for a signal beam waist diameter of 340  $\mu\text{m}$ , the calculation gave a maximum extracted power of 27 W. As the absorbed pump power was 50 W at 808 nm in our experiment, the maximum extracted power at 1064 nm was theoretically 38 W (by taking the quantum defect in account). Therefore, an estimation of the overlap between the signal and the pump can be given by the ratio  $27/38 = 71\%$ .

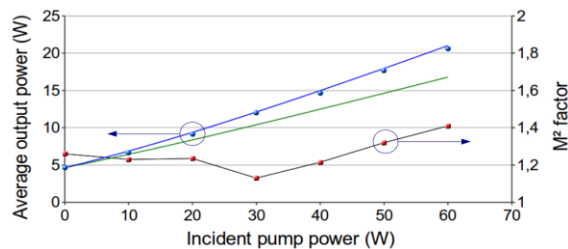


Fig. 9. Output average power (blue dots) and  $M^2$  factor (red square) versus the incident pump power with the PicoSpark™ in a simple pass configuration. This lines in blue and green are simulated output power for the 50 mm long single crystal fiber (blue) and for a 30 mm long sample (green).

We studied the saturation of the gain inside the single-crystal fiber amplifier. Figure 10 shows the gain versus the incident average power for a pump power of 60 W. The gain was strongly saturated for signal powers higher than 1 W with a minimum value of 4 (at 5 W of incident signal). We also tried a second pass but the output power was not higher than in one pass, showing that the extraction was nearly complete after a single pass.

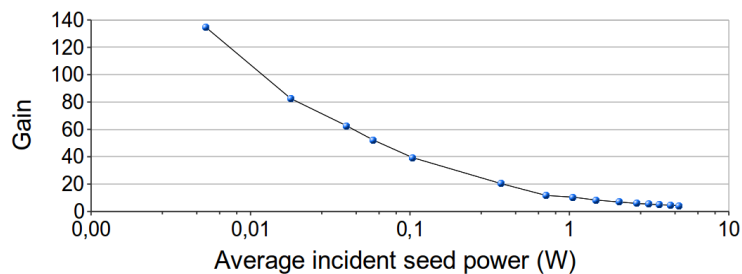


Fig. 10. Gain versus the average incident signal power with the PicoSpark™ laser source in a simple pass configuration for 60 W of incident pump power.

## 5. Nd:YAG single-crystal fiber as energy amplifier

With a long fluorescence lifetime (230  $\mu\text{s}$ ), Nd:YAG is more adapted to store energy than Nd:YVO<sub>4</sub> (lifetime of 100  $\mu\text{s}$ ). It is then interesting to investigate the potential of Nd:YAG single-crystal fiber as energy amplifier for a passively Q-switched microlaser operating at low repetition rate. The seeding source is this time a Powerchip<sup>TM</sup> laser source from Teem Photonics. It delivered 450 ps pulses at the frequency of 1 kHz with an energy of 80  $\mu\text{J}$  and an average power of 80 mW at 1064 nm. We used the setup 2 to carry out the experiment. The optics for the signal were modified in order to increase the beam diameter of the signal up to 480  $\mu\text{m}$  and to reduce the fluence on the surfaces of the single-crystal fiber.

As the time interval between signal pulses was 1 ms, far larger than the lifetime, it was possible to operate the pump diode in quasi-continuous wave in order to reduce the average pump power. This allowed to reduce the crystal temperature and to suppress the small spectral shift visible on the Fig. 3. After optimization, we chose a duty cycle of 0.31 with pump pulses of 310  $\mu\text{s}$ . The pump was synchronized on the pumping diode of the Powerchip<sup>TM</sup> laser which was also operating at 1 kHz.

The Fig. 11 shows the output energy obtained in a single pass. At maximum pump power, the single-crystal fiber delivered pulses with an energy of 1.55 mJ, a pulse duration of 450 ps corresponding to a peak power of 3.4 MW.

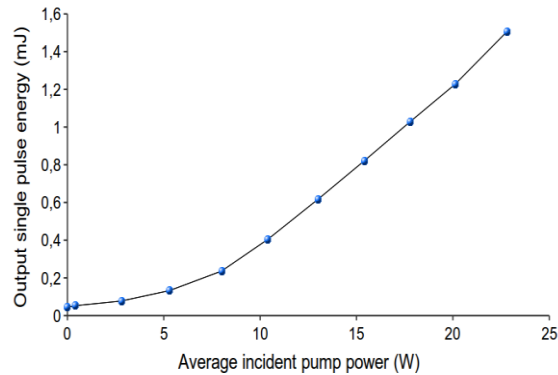


Fig. 11. Output energy in single pass configuration versus the pump power.

The Fig. 12 shows the results in double pass configuration. This time, the output energy reached 2.7 mJ for a pulse duration that remained at 450 ps as shown on the Fig. 13. The peak power was 6 MW. The  $M^2$  factor of the incident beam was 1.2. The output  $M^2$  factor is presented on the Fig. 12 versus the pump power. It remained below 1.35, at a lower value than the  $M^2$  presented in the previous section, showing the interest to operate in quasi-continuous wave in this case.

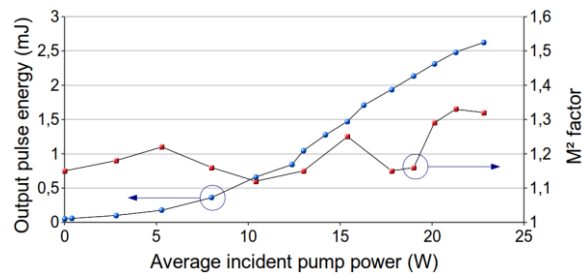


Fig. 12. Output energy in double pass configuration versus the pump power (left).  $M^2$  factor versus the pump power (right).

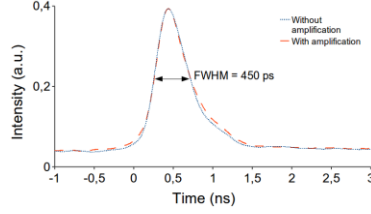


Fig. 13. Duration of the output pulses after two pass amplification and without amplification (recorded with a 4GHz single shot oscilloscope).

As the peak power was very high, we looked after any non-linear effects that may appear in the single crystal fiber. No temporal deformation was visible on the pulse profile shown on the Fig. 13. We also carried out a spectral analysis with a Fabry-Perot interferometer with a free spectral range of 1.6 GHz to investigate possible changes in the signal spectrum. There was no visible variation on the interference ring pattern with and without amplification, indicating no sign of self-phase modulation effect. Indeed, we estimated that the B-integral was below 0.38 for the first pass and below 0.67 for the second pass. This means that the cumulative B-integral for the two passes was below 1, far from deleterious nonlinear effects [19].

Concerning spatial nonlinear effects, the self-focusing threshold (1.44 MW for Nd:YAG [20]) is lower than the peak powers obtained. However, with the beam diameter of 480  $\mu\text{m}$  (measured on the output face of the crystal after the second pass), we can estimate the focal length of the nonlinear lens induced to be in the order of 130 mm, larger than the length of the single-crystal fiber. This explains why self-focusing is not a limiting effect in this configuration.

This beam diameter led to an energy density of 1.46  $\text{J}/\text{cm}^2$  on the crystal output face. This value remained below the damage threshold of the crystal antireflection coatings estimated to be at 2  $\text{J}/\text{cm}^2$ .

## 6. Discussion and conclusion

In order to estimate the performance of the Nd:YAG single-crystal fiber, we calculate the extraction efficiency. For the high repetition rate lasers (described in sections 3 and 4), It was given by a ratio of powers:

$$\eta_{extr} = \frac{\overline{P_{out}} - \overline{P_{in}}}{\overline{P_{pump}}} \quad (1)$$

where  $P_{pump}$  is the pump power delivered by the laser diode,  $P_{in}$  and  $P_{out}$  are the average power of the signal before and after amplification. Note that  $P_{in}$  and  $P_{pump}$  are taken directly at the output of the lasers in order to take all the losses into account.

In case of the low repetition rate laser operating at 1 kHz (section 5), we prefer to express the extraction efficiency as a ratio of energies since the pumping was in quasi-continuous operation:

$$\eta_{extr} = \frac{E_{out} - E_{in}}{E_{sto}} \quad (2)$$

where  $E_{in}$  and  $E_{out}$  are the signal energy before and after amplification respectively.  $E_{sto}$  is the energy stored by the Nd:YAG during the pump pulse. It can be expressed by:

$$E_{sto} = \frac{\lambda_p}{\lambda} P_{pump} \tau \cdot \left(1 - e^{-\frac{t}{\tau}}\right) \quad (3)$$

where  $\lambda_p$  and  $\lambda$  are the pump and the signal wavelength respectively,  $\tau$  is the fluorescence lifetime and  $t$  is the pumping duration.

The performances are summarized on the Table 1, following the seed laser and the number of passes. At high repetition rates (for seed#1 and seed#2), the average power is the highest ever produced by an Nd doped amplifier used for amplification of passively Q-switched pulses. It is also worth to note that the extraction efficiency is twice the one obtained with a Nd:YVO<sub>4</sub> amplifier of PQS laser, having an output power of 10 W [7]. Hence, despite its lower cross section, Nd:YAG single-crystal fiber overcomes bulk Nd:YVO<sub>4</sub> amplifiers reported in the literature for high repetition rate pulses. At low repetition rate, which is particularly well adapted for Nd:YAG, the extraction efficiency overcomes the previous performance by a factor of 5.

Compared to fiber amplifiers the extraction efficiency is lower but one has to mention the simplicity of the Nd:YAG single-crystal fiber amplifier, with only one gain medium, with low energy fluence (J/cm<sup>2</sup>), with a linearly polarized output, without amplified spontaneous emission and without nonlinear effects to manage. One has to mention that the extraction efficiency for seed#2 reaches the level obtained in a fiber amplifier [12] for a pump power level of 60 W. For the same degree of complexity (ie only one amplifier), the Nd:YAG single-crystal fiber outperforms the energy and the peak power by a factor higher than two with respect to fiber amplifier [11].

**Table 1. Summary of the Performance Obtained with the Nd:YAG Single-Crystal Fiber Amplifier\***

	Simple pass	Double pass
<b>Seed#1</b>	$\eta_{\text{extr}} = 8.4\%$	$\eta_{\text{extr}} = 20.2\%$
100 kHz, 350 mW <sub>av</sub> , 3.5 $\mu$ J, 1 ns	5.4 W <sub>av</sub> , 54.5 $\mu$ J, 54.5 kW <sub>peak</sub>	12.5 W <sub>av</sub> , 126 $\mu$ J, 126 kW <sub>peak</sub>
<b>Seed#2 "PicoSpark™"</b>	$\eta_{\text{extr}} = 25.8\%$	
42 kHz, 5 W, 120 $\mu$ J, 1 ns	20.5 W <sub>av</sub> , 488 $\mu$ J, 488 kW <sub>peak</sub>	
<b>Seed#3 "Powerchip™"</b>	$\eta_{\text{extr}} = 18.4\%$	$\eta_{\text{extr}} = 33.9\%$
1 kHz, 80 mW, 80 $\mu$ J, 0.45 ns	1.5 W <sub>av</sub> , 1.5 mJ, 3.3 MW <sub>peak</sub>	2.7 W <sub>av</sub> , 2.7 mJ, 6 MW <sub>peak</sub>

\*W<sub>av</sub> refers to the average power, W<sub>peak</sub> refers to the peak power.

It has also worth to mention the flexibility of the Nd:YAG single-crystal fiber. Our work shows that the same experimental setup is able to produce performance overcoming the previous bulk amplifiers in very different regimes: high gain amplifier, power amplifier, energy amplifier. Moreover, the design is very simple, with only one gain medium and a maximum of two passes. The curves presenting the output energy or the average output power versus the pump power show not sign of saturation coming from parasitic spectroscopic and thermal effects. This means that a power scaling is possible either by increasing the pump power or by both sides pumping. Concerning the energy amplifier, the limit for energy scaling will come from the energy fluence on the single-crystal fiber coating. One way to solve this problem is to work with a Brewster angle cut single-crystal fiber.

In conclusion, Nd:YAG single-crystal fibers give solutions to the problems occurring in bulk crystals and in fibers for amplification of pulses combining high peak power and high average power. Nd:YAG single-crystal fibers bring a significant breakthrough for amplifiers of passively Q-switched microlasers. They have a strong potential for power and energy scaling.